Available online at www.sciencedirect.com
SCIENCE DIRECT®
Chemistry and Physics of Lipids 135 (2005) 213–221
CPL
CHEMISTRY AND PHYSICS OF LIPIDS
www.elsevier.com/locate/chemphyslip

Influence of the curvature on the water structure in the headgroup region of phospholipid bilayer studied by the solvent relaxation technique

Jan Sýkora [a], Piotr Jurkiewicz [a,b], Richard M. Epand [c], Ruud Kraayenhof [d], Marek Langner [b], Martin Hof [a,*]

[a] *J. Heyrovský Institute of Physical Chemistry, Academy of Sciences of the Czech Republic, Dolejškova 3, CZ-18223 Prague 8, Czech Republic*
[b] *Institute of Physics, Wroclaw University of Technology, Wybrzeze Wyspianskiego 27, 50-370 Wroclaw, Poland*
[c] *Department of Biochemistry, McMaster University Health Sciences Centre, 1200 Main Street West, Hamilton, Ont., Canada L 8N 3Z 5*
[d] *Institute of Molecular Biological Sciences, BioCentrum Amsterdam, Vrije Universiteit, De Boelelaan 1087, 1081HV Amsterdam, The Netherlands*

Received 11 January 2005; received in revised form 3 March 2005; accepted 7 March 2005
Available online 11 April 2005

Abstract

Solvent relaxation (SR) in 1,2-dioleoyl-palmitoyl-*sn*-glycero-3-phosphocholine (DOPC) unilamellar vesicles of different size was probed by 6-hexadecanoyl-2-(((2-(trimethylammonium)ethyl)methyl)amino)naphthalene chloride (Patman), 6-propionyl-2-dimethylaminonaphthalene (Prodan) and 4-[(*n*-dodecylthio)methyl]-7-(*N*,*N*-dimethylamino)-coumarin (DTMAC). Patman probes the amount and mobility of the bound water molecules located at the carbonyl region of the bilayer. Membrane curvature significantly accelerates the solvent relaxation process, but does not influence the total Stokes shift, showing that membrane curvature increases the mobility, without affecting the amount of water molecules present in the headgroup region. This pattern was also verified for other phosphatidylcholines. Prodan is located in the phosphate region of the bilayer and probes a more polar, mobile and heterogeneous environment than Patman. The influence of membrane curvature on SR probed by Prodan is similar, however, less pronounced compared to Patman. DTMAC (first time used in SR) shows a broad distribution of locations along the *z*-axis. A substantial amount of the coumarin chromophores face bulk water. No effect of curvature on SR probed by DTMAC is detectable.

Keywords: Patman; Prodan; Coumarin; Bound water; Time-resolved emission spectra (TRES); *t*(0)-Estimation

1. Introduction

It has been reported in recent work that a change in membrane curvature accompanies membrane fu-

* Corresponding author.
E-mail address: hof@jh-inst.cas.cz (M. Hof).

0009-3084/$ – see front matter © 2005 Elsevier Ireland Ltd. All rights reserved.
doi:10.1016/j.chemphyslip.2005.03.003

sion (Tamm et al., 2003), which many biological processes are based on. For instance, the formation of tubules and vesicles inside cells (Zimmerberg and McLaughlin, 2004), the formation of new organelles and enveloping of viruses (Huttner and Zimmerberg, 2001) as well as protein binding (Chao et al., 2002) might be realized via intermediates featuring "membrane bent structures". Efforts are taken to find possible mechanisms of these processes and the characterization of the physical properties of the deformed bilayer state appears to be a key task. Thus, we decided to exploit the advantages of the solvent relaxation (SR) technique and to monitor the changes of the water structure in the interface and headgroup region of phospholipid bilayers of different curvature. The SR approach in general gives direct information on the dynamics and polarity in supramolecular assemblies, in our case in particular regions of unilamellar vesicles. It inspects time-resolved emission (fluorescence) spectra (TRES) of probes, which are well defined located in these particular regions of the bilayer. Electronic excitation leads to an abrupt change in charge distribution of these dyes and is initiating the dynamic process of reorganization of the dyes microenvironment. This so-called solvent relaxation process leads to a dynamic Stokes shift of the TRES. The time course of this SR process is monitored through the observation of the position of the emission maximum frequency, $\nu(t)$, of the recorded TRES and contains information on the organization of the dyes microenvironment.

The important issue of this kind of study is to guarantee that the used probes are well defined located in the particular region of the bilayer. In our work, three dyes that fulfill the location criteria under the applied experimental conditions were chosen for probing the solvation dynamics in the headgroup and interface region. Firstly, the chromophore of Patman is located in the carbonyl region (Hutterer et al., 1996) where all the water molecules are bound to the functional groups (Sýkora et al., 2002a). In a series of applications of the SR method in bilayer characterization, the localization of Patman (Fig. 1) proved to be invariant to parameters like lipid composition (Hutterer et al., 1997a,b; Sheynis et al., 2003), temperature (Hutterer et al., 1996, 1997a), addition of ethanol (Hutterer and Hof, 2002) or protein binding (Hutterer et al., 1997b; Sheynis et al., 2003). Secondly, Prodan is located closer to the interface in the phosphate region (Fig. 1) where the solvation dynamics is faster than in the region probed by Patman (Hutterer et al., 1996; Sýkora et al., 2002a). In addition, the phosphate group is more hydrated, which results in high micropolarity of Prodan microenvironment. It has been recently shown that factors like hydrostatic pressure (Chong et al., 1989) or addition of ethanol (Hutterer and Hof, 2002) partially relocalizes Prodan to a more hydrated and less structured localization. However, in the herein investigated DOPC vesicles, the inspection of the TRES indicates that the Prodan molecules are located at or close to a single main location. Finally, we are using DTMAC, a coumarin-like dye. As already estimated from steady-state data (Epand et al., 1996), the SR data presented herein indicates that the chromophore of DTMAC is found to be located similar to Prodan at the interface region (Fig. 1). Since DTMAC is used in SR studies for the first time, a detailed description of the estimation of the Franck–Condon spectrum ("time-zero spectrum") of DTMAC in vesicles is given. The deformation of the bilayer was simulated by different dimensions of used vesicles, namely 20 nm large sonicated small unilamellar vesicles (SUVs) and 200 nm large extruded large unilamellar vesicles (LUVs). In case of LUVs, the difference between the ratio of the inner and outer surface is approximately 1, whereas in case of SUVs it falls down to 0.5, which naturally influences the packing of the bilayer. In order to reveal these effects, we decided to label either both membrane bilayer leaflets or the outer leaflet alone assuming that the selective labeling will affect the solvation dynamics in case of SUVs more dramatically than in case of LUVs.

2. Materials and methods

Probes 6-hexadecanoyl-2-(((2-(trimethylammonium)ethyl)methyl)amino)naphthalene chloride (Patman) and 6-propionyl-2-dimethylaminonaphthalene (Prodan) were purchased from Molecular Probes and were used without any further purification. 4-[(*n*-Dodecylthio)methyl]-7-(*N*,*N*-dimethylamino)-coumarin (DTMAC) was synthesized as described in (Sterk et al., 1997) and purified by HPLC. Lipids: 1,2-dioleoyl-palmitoyl-*sn*-glycero-3-phosphocholine (DOPC), 1,2-dimyristoyl-*sn*-glycero-3-phosphocholine (DMPC), 1,2-oleoyl-palmitoyl-*sn*-glycero-3-phosphocholine (OPPC) and 1,2-palmitoyl-

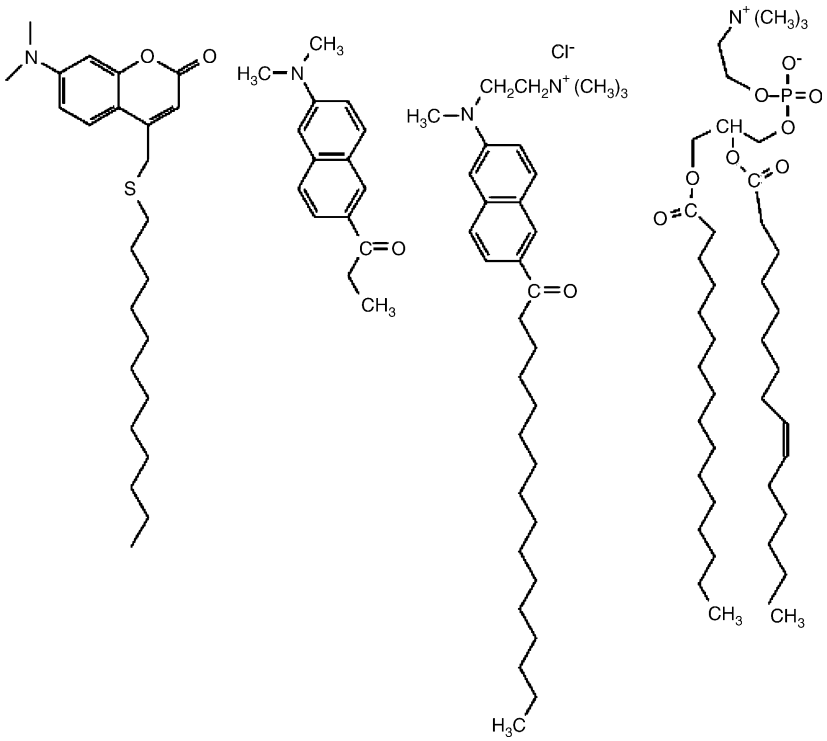

Fig. 1. Structures of the used probes. From the left: DTMAC, Prodan, Patman and a molecule of phosphatidyl choline.

oleoyl-*sn*-glycero-3-phosphocholine (POPC) were supplied from Avanti Lipids. All solvents of spectroscopic grade were purchased from Merck. The preparation of PC SUVs was carried out via sonication (Hope et al., 1986) and LUVs were prepared by the extrusion with 200 nm filters (Hope et al., 1986). Absorption spectra were recorded on a Perkin-Elmer Lambda 19 spectrometer. Fluorescence spectra and decays were recorded on a Fluorolog 3 steady-state spectrometer (Jobin Yvon) and on an IBH 5000 U SPC equipment, respectively. Decay kinetics were recorded by using an IBH laser diode NanoLED 11 (370 nm peak wavelength, 80 ps pulse width, 1 MHz repetition rate) and a cooled Hamamatsu R3809U-50 microchannel plate photomultiplier. The primary data consist of a set of emission decays recorded at a series of wavelengths spanning the steady-state emission spectrum. The time-resolved emission spectra (TRES) were gained by the spectral reconstruction method (Horng et al., 1995). Full width at half maxima (FWHM) and emission maxima ($\nu(t)$) profiles of the reconstructed TRES were yielded from log-normal fitting of the time-resolved emission spectra. The obtained correlation functions ($C(t) = (\nu(t) - \nu(\infty))/\Delta\nu$) were fitted with a sum of exponentials as described in (Horng et al., 1995). The size distributions of prepared vesicles were checked by dynamic light scattering (DLS). The light scattering setup (ALV, Langen, Germany) consists of a 633 nm He–Ne laser, an ALV CGS/8F goniometer, an ALV High QE APD detector and an ALV 5000/EPP multibit, multitau autocorrelator. The solutions for measurements were filtered through 0.45 μm Acrodisc filters. Analysis of the data was performed by fitting the experimentally measured normalized intensity autocorrelation function. The results demonstrate that both SUVs and LUVs feature a narrow size distribution with its maximum of diameter at 20 nm and 200 nm, respectively. Moreover, no additional peaks resulting from the formation of aggregates were detected.

3. Results and discussion

3.1. Time-zero (t(0))estimation

To determine the correlation function $C(t)$, one needs to know the position $\nu(t=0)$ of the so called "time-zero" spectrum—the hypothetical fluorescence emission spectrum of the molecules which are vibrationally relaxed but emit before any nuclear solvent motion has occurred. Experimental determination of $\nu(0)$ based on extrapolation of the observed spectra back to $t=0$, is strongly affected by the time resolution of the instrumentation and often leads to significant errors in calculated solvation times (Fee and Maroncelli, 1994). Thus, as demonstrated for a series of membrane labels, a valid "time-zero" estimation independent of the given experimental time resolution is a pre-requisite for quantitative SR studies (Hutterer and Hof, 2002; Sýkora et al., 2002a,b). While this procedure has already been performed for both Patman and Prodan (Sýkora et al., 2002a), it is not documented for DTMAC so far. The method used in this study, described by Fee and Maroncelli (1994) is based only on the steady-state spectra measured in polar and non-polar solvents and is independent of the time resolution of the experiment. The absorption and fluorescence emission spectra of DTMAC in non-polar reference solvent (cyclohexane) were measured and normalized to obtain lineshape functions of absorption, $g(\nu)$, and emission, $f(\nu)$. Absorption spectra, $A(\nu)$, were measured for all the liposome samples. Assuming that the spectra of individual molecules in different environments differ only by an overall frequency shift, δ, the site distribution Gaussian function, $p(\delta)$, was calculated by fitting its convolution with $g(\nu)$ to the absorption spectrum $A(\nu)$. Once properly fitted, the site distribution profile allows calculation of the "time-zero" spectrum from the lineshape functions (see Fig. 2). The method was implemented in C language using a non-linear least-squares fitting routine. All the spectra were measured at room temperature. The estimated position of the DTMAC "time-zero" spectrum in terms of its maximum for all liposome systems was $\nu(0) = 22750\,\mathrm{cm}^{-1}$.

The SR monitored by the three dyes has been characterized for four different vesicle–dye preparations, denoted by "SUV addition before", "SUV addition after", "LUV addition before" and "LUV addition after", respectively. For example, the notation "SUV addition before" is referred to the sample which contains SUVs and the dye was added before the unilamellar vesicles were prepared by sonication, thus enabling labeling of both bilayer leaflets, and "LUV addition after" stands for the extruded vesicles that were labeled after the formation of the LUVs resulting in the selective labeling of the outer leaflet. The dyes were chosen in order to monitor SR in different regions of the headgroup part of the phospholipid bilayer.

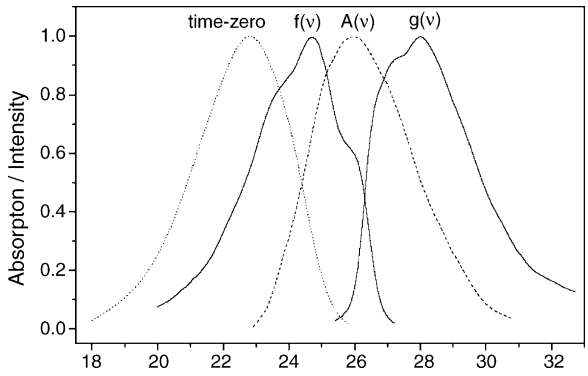

Fig. 2. The estimated time-zero fluorescence emission spectrum of DTMAC (dotted line) and the spectra used for its calculation: absorption, $g(\nu)$, and emission, $f(\nu)$, lineshape functions (solid lines) obtained from data measured in cyclohexane and absorption spectrum, $A(\nu)$, of the dye in DOPC LUVs (dashed line). All the spectra were measured in the room temperature. See text for details of the estimation procedure. DTMAC time-zero spectra calculated for the remaining liposomes compositions were almost identical.

To estimate the effect of flip–flop motion of the used dyes, a sample of "SUV addition after" labeled with Prodan was re-measured after 24 h and no changes were detected. The absence of any differences in case of Prodan makes the influence of the flip–flop mechanism for DTMAC and Patman unlikely since they are more tightly attached to the bilayer. Besides, more details on the effect of various vesicle preparations for Prodan and Patman can be found in (Hutterer et al., 1996). The discussion will be firstly focused on Patman, which is supposed to be located at the region of carbonyl residues (Hutterer et al., 1996).

3.2. Solvent relaxation probed by Patman in LUVs and SUVs composed of DOPC

Before discussing the difference between the four various vesicle preparations, we would like to draw the following general conclusions for the investigated

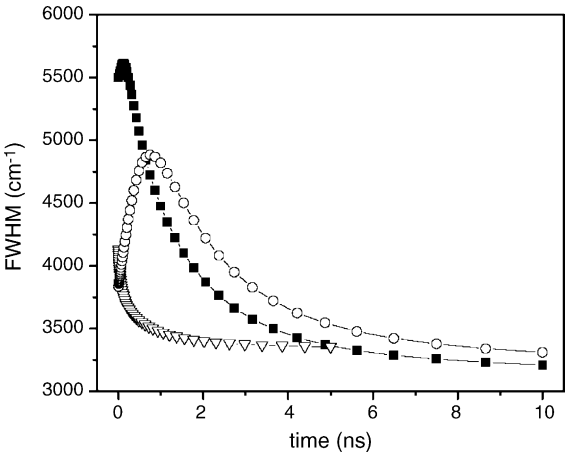

Fig. 3. The FWHM of the TRES as a function of time after excitation for Patman (open circles), Prodan (filled squares) and DTMAC (open triangles) incorporated in DOPC LUVs during their preparation (addition before). Data ware measured at room temperature.

Patman systems. A comparison of the $\Delta\upsilon$ values determined by using the $\upsilon(0)$ values determined by the "time-zero spectrum estimation" with those obtained exclusively by TRES reconstruction shows that the solvent relaxation probed by Patman is practically captured by our equipment providing about 50 ps time-resolution. This conclusion is confirmed by the time evolution of the FWHM (Fig. 3). The observed profiles for Patman prove that during the lifetime of the excited state solvent relaxation completes and the whole relaxation process is occurring on the nanosecond timescale. The absence of a significant "ultrafast" component demonstrates that the chromophores of the dyes located within the headgroup region are not in contact with "bulk" water. Moreover, the FWHM time profiles give evidence that the ensemble of Patman molecules is located at or close to a single main location. The fact that those profiles are practically identical for all systems implies that no severe relocalization of Patman happened due to variation of the vesicle preparation. The basic characteristic, which is proportional to the polarity of the dye microenvironment, is the overall Stokes shift $\Delta\upsilon$. As it is obvious from Table 1, different vesicle preparations do not lead to significant changes in the $\Delta\upsilon$ values probed by Patman. Thus, we assume that the stronger curvature does not lead to changes in the degree of hydration within the glycerol region of the bilayer. Unlike the micropolarity, significant changes in the kinetics of solvent relaxation are evident. Both the average relaxation time and the integrated relaxation time are smallest for the "SUV addition after". Besides, the values for both "LUV addition before and after" and "SUV addition before" remain constant within the experimental error at given time resolution. This indicates that the changes in the packing of phospholipids take place when the outer leaflet is more bent and the hydrated functional groups naturally become more mobile. When both leaflets in the curved SUVs are labeled, the tighter headgroup packing of the inner layer apparently compensates this effect. If one wishes to quantify the SR kinetics in the inner leaflet of SUV, one has to be aware that the outer leaflet contains two times more molecules of the dye and thus, the contribution of the SR from the outer leaflet is dominating the obtained values. However, as the SR kinetics appears to be slower in "SUV addition before" than

Table 1
Characteristics of the solvent relaxation process in DOPC liposomes probed by Patman

Vesicle preparation[a]	$\Delta\nu$ (cm^{-1})[b]	τ_1 (ns)[c] [A_1]	τ_2 (ns)[c] [A_2]	τ_3 (ns)[c] [A_3]	τ_{av} (ns)[d]	τ_r (ns)[e]	Observed (%)[f]
SUV before	3450	<0.05 [0.15]	0.53 [0.35]	1.68 [0.50]	1.46	1.22	85
SUV after	3500	<0.05 [0.14]	0.42 [0.46]	1.52 [0.40]	1.24	0.91	84
LUV before	3450	<0.05 [0.15]	0.80 [0.58]	2.11 [0.27]	1.51	1.19	84
LUV after	3500	<0.05 [0.17]	0.50 [0.47]	1.90 [0.36]	1.52	1.14	86

[a] Vesicle–dye preparations—see text for notion details.
[b] $\Delta\nu = \nu(0) - \nu(\infty)$; $\nu(0)$ estimation—see text; $\nu(\infty)$ were obtained by TRES reconstruction.
[c] Solvent relaxation time constants resulting from (multi)exponential fitting of the $C(t)$ functions.
[d] Average relaxation time: $\tau_{av} = \frac{A_1\tau_1^2 + A_2\tau_2^2 + A_3\tau_3^2}{A_1\tau_1 + A_2\tau_2 + A_3\tau_3}$.
[e] Integral relaxation time: $\tau_r = \int_0^\infty C(t)\,dt$.
[f] Percentage of observed SR process obtained by comparison of the $\Delta\nu$ values calculated using the $\nu(0)$ values from the time-zero spectrum estimation with those obtained exclusively by TRES reconstruction.

"SUV addition after", the solvation dynamics of the inner leaflet of SUVs must be significantly slower than the given "averaged" values.

The obtained correlation functions were best fitted with a sum of three exponentials. This pattern appears to be a rather general feature for headgroup labels in DOPC vesicles (see also for *N*-palmitoyl-3-aminobenzanthrone (Sýkora et al., 2002b) and DMPC vesicles (data for Prodan, Patman and DTMAC not shown (Sýkora et al., 2002b)). However, at the present stage of knowledge we consider detailed discussion on the origin of these individual components as speculative.

3.3. Solvent relaxation probed by Prodan and DTMAC in LUVs and SUVs composed of DOPC

Despite of the fact that Prodan is one of the most popular membrane probes, lipid experiments on hydrostatic pressure (Chong et al., 1989), addition of ethanol (Hutterer and Hof, 2002) as well as comparison with the behavior of other chromophores (Klymchenko et al., 2004) led to a recent debate whether Prodan is indeed located at or close to a single main location within phospholipid bilayers or if re-localization phenomena leading to a second main location had to be considered. As we have recently demonstrated when investigating the solvent relaxation behavior of the newly developed membrane label *N*-palmitoyl-3-aminobenzanthrone in different phase states of phospholipids bilayers (Sýkora et al., 2002b), the inspection of the time course of the FWHM is an excellent tool to distinguish between those two options. As shown in Fig. 3, the FWHM profile of Prodan in DOPC vesicles shows only one maximum, indicating that in the investigated particular systems the ensemble of Prodan molecules is indeed distributed around one most probable location. The higher values of FWHM for Prodan than for Patman imply that its microenvironment is more heterogenous than for Patman. The faster time course of the solvent relaxation is a consequence of the closer localization of Prodan towards the interface. Both findings are consistent with published data demonstrating a preferential location of Prodan in the phosphate region of phosphatidylcholine bilayers in the liquid-crystalline phase (Hutterer et al., 1996) in the absence of hydrostatic pressure and alcohols. The partially missing raising edge in the FWHM profile shows that a small, but significant part of the SR process is occurring on a time scale faster than 50 ps. Since our approach does not give fully quantitative information on this small "ultrafast" SR event, we cannot exclude that a small fraction within the ensemble of Prodan molecules attached to DOPC bilayers is "seeing" bulk water. For all four measured systems, the FWHM curves were found almost identical (data not shown), demonstrating that the higher curvature does not lead to different partitioning of Prodan inside the bilayer.

DTMAC is located most outside of the bilayer and the result corresponds to such a location. It features somewhat faster solvation dynamics in comparison to Prodan. The time evolution of FWHM does not show any maximum suggesting that a substantial part of the relaxation process is not captured. Indeed (see Table 3), up to 40% SR happens beneath the given time resolution. Nevertheless, the 3-exponentional fitting of the correlation function yielded satisfactory results as for previously discussed dyes. However, the contribution of the fastest component (<0.05 ns) is larger than for both Prodan and Patman providing another proof that compared to Prodan, a larger percentage of the DTMAC molecules are in contact with bulk water. Similar as for Prodan, the higher curvature did not lead to any significant changes in the course of the FWHM profiles (data not shown).

As mentioned in the previous sections, we compare three dyes that are believed to be located at gradual depths of the headgroup region of the phospholipid bilayers: Patman is the deepest located at the glycerol region "seeing" only bound water molecules. Prodan is located close to the interface approximately at the hydrated phosphate groups (Hutterer et al., 1996) and possibly a small part of the molecules are in contact with "unbound" water molecules. DTMAC is apparently located similar to Prodan (Fig. 4). However, the sub-picosecond component is most significant among these three dyes. This indicates a rather broad distribution of locations along the *z*-axis of the bilayer with the consequence that a substantial amount of the coumarin chromophores might face bulk water molecules. As it is obvious from Tables 1–3, the overall Stokes shift remains the same regardless of the deformation of the bilayer for all three dyes. This means that the higher curvature does not cause any changes in the degree of hydration of the probe and the polarity of the dye microenvironment remains constant.

Table 2
Characteristics of the solvent relaxation process in DOPC liposomes probed by Prodan

Vesicle preparation[a]	$\Delta\nu$ (cm^{-1})[b]	τ_1 (ns)[c] [A_1]	τ_2 (ns)[c] [A_2]	τ_3 (ns)[c] [A_3]	τ_{av} (ns)[d]	τ_r (ns)[e]	Observed (%)[f]
SUV before	4075	<0.05 [0.22]	0.20 [0.50]	1.07 [0.25]	0.81	0.53	75
SUV after	4075	<0.05 [0.28]	0.21 [0.42]	0.98 [0.30]	0.77	0.47	72
LUV before	4075	<0.05 [0.24]	0.24 [0.39]	0.99 [0.37]	0.82	0.60	74
LUV after	4025	<0.05 [0.28]	0.20 [0.42]	1.02 [0.30]	0.82	0.52	72

For footnotes (a–f), see Table 1.

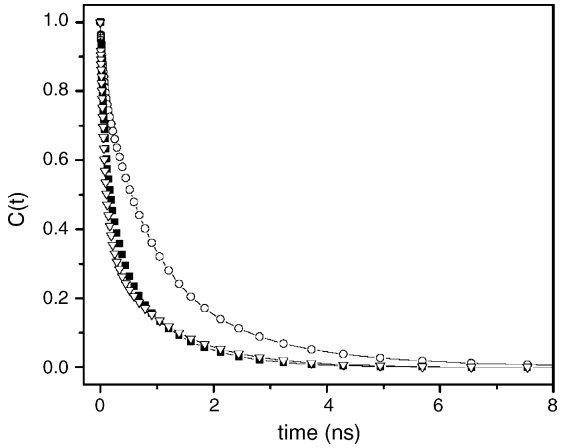

Fig. 4. Correlation functions for Patman (open circles), Prodan (filled squares) and DTMAC (open triangles) incorporated in DOPC LUVs during their preparation (addition before). Data were measured at room temperature.

On the contrary, the relaxation times show that there are apparent differences in the mobility of the dye microenvironment when the bilayer is more bent. The most significant differences were observed for Patman, where the solvation dynamics was about 15% faster for "SUV addition after" than for the other systems. When moving towards the interface region, the difference in the SR behavior is pronounced no more so clearly. In case of Prodan, approximately 5% faster SR for "SUV addition after" is found, and for DTMAC, the data show no clear trends.

To verify that the above drawn conclusions for the vesicles composed of DOPC are valid in general, the attention was also paid to DMPC at two temperatures and to mixed chain isomers OPPC and POPC at 20 °C. Patman was chosen as the appropriate dye for the largest effects were found for DOPC vesicles using this probe. The experiments were only carried out for SUVs.

The SR experiments for DMPC SUV were carried out only for SUVs at 30 °C and 50 °C above the main phase transition temperature, T_c, which is 21 °C (Koynova and Caffrey, 1998). The latter conditions did not exhibit an exception to the pattern discussed for DOPC. However, at the temperature closer to the phase transition the DMPC vesicles ("SUV addition before" and "SUV addition after") show a different pattern (Table 4). To explain this result observed at 30 °C, we inspected the time evolutions of FWHM for SUVs at both temperatures, which were found to be significantly broadened in case of 30 °C (data not shown). This implies that the microenvironment of Patman is more heterogeneous suggesting the idea that some coexistence of fluid and gel phases takes place. This hypothesis is consistent with data obtained with differential scanning calorimetry showing that the transition width is generally broader for SUVs (Heerklotz and Seelig, 2002). Moreover, in a recent solvent relaxation study using a benzanthrone-like dye it was shown that indeed, 9 °C above the phase transition temperature in DMPC SUV some phase coexistence is present (Sýkora et al., 2002a,b). Such coexistence can certainly affect

Table 3
Characteristics of the solvent relaxation process in DOPC liposomes probed by DTMAC

Vesicle preparation[a]	$\Delta\nu$ (cm^{-1})[b]	τ_1 (ns)[c] [A_1]	τ_2 (ns)[c] [A_2]	τ_3 (ns)[c] [A_3]	τ_{av} (ns)[d]	τ_r (ns)[e]	Observed (%)[f]
SUV before	2200	<0.05 [0.41]	0.22 [0.32]	1.19 [0.23]	0.94	0.49	69
SUV after	2200	<0.05 [0.33]	0.21 [0.44]	1.17 [0.23]	0.91	0.48	61
LUV before	2150	<0.05 [0.31]	0.14 [0.35]	1.14 [0.34]	0.97	0.49	75
LUV after	2200	<0.05 [0.35]	0.18 [0.33]	1.18 [0.32]	0.92	0.49	71

For footnotes (a–f), see Table 1.

Table 4
Basic characteristics of the solvent relaxation process in DMPC, POPC and OPPC liposomes probed by Patman

Vesicle preparation	DMPC[a]		DMPC[b]		POPC[c]		OPPC[d]	
	$\Delta\nu$ (cm^{-1})	τ_r (ns)	$\Delta\nu$ (cm^{-1})	τ_r (ns)	$\Delta\nu$ (cm^{-1})	τ_r (ns)	$\Delta\nu$ (cm^{-1})	τ_r (ns)
SUV before	3350	2.29	3350	0.82	3400	1.87	3400	2.02
SUV after	3400	2.39	3350	0.73	3450	1.40	3450	1.66

[a] Measured at 30 °C (T_c = 21 °C).
[b] Measured at 50 °C (T_c = 21 °C).
[c] Measured at 20 °C (T_c = −2.6 °C).
[d] Measured at 20 °C (T_c = −9.3 °C).

the solvent relaxation kinetics and thus, be the reason for the different pattern observed.

As far as POPC and OPPC vesicles are concerned, "SUVs addition before" performs the slowest solvation dynamics following again the trends observed for DOPC vesicles. Nevertheless, this system is interesting from another point of view. It was proved that the solvation dynamics becomes faster as the experimental temperature moves further from the phase transition temperature, T_c (Hutterer et al., 1997a,b,c). However, it is no more valid for the pair of isomers OPPC (T_c = −9.3 °C) and POPC (T_c = −2.6 °C) (Koynova and Caffrey, 1998). Apparently, OPPC should feature faster solvation dynamics than POPC. Surprisingly, the SR kinetics is slower in case of OPPC as obvious from Table 4. At the relative temperature to the phase transition, the difference in the relaxation times even reaches 30%. This fact shows that the mere swapping of the acyl chains affects the alignment of the polar headgroup region. In order to get additional information on the change in hydration of the headgroup region of the chain isomers, NMR studies will be performed (Finer and Darke, 1974; Lindblom et al., 1976; Westlund, 2000).

4. Conclusions

In conclusion, the higher curvature does lead to the different packing of the phospholipid bilayer; however, the effect is not as dramatic as estimated in a single-wavelength study using a dye with a rather undefined location (Hof et al., 1994). It seems that the degree of hydration is not modified by the higher curvature at all; nevertheless, the mobility of the dye microenvironment is increased when the bilayer is more bent. This trend is clearly visible in the glycerol region where the bound water is present exclusively. Approaching the interface region, which is accompanied by the gradual increase in a content of free water, these tendencies become less and less apparent.

Acknowledgements

Financial support by the Czech Academy of Sciences (M.H. and P.J. via A400400503) and the Grant Agency of the Czech Republic (J.S. via 203/05/2308) is gratefully acknowledged.

References

Chao, H., Martin, G.G., Russell, W.K., Waghela, S.D., Russell, D.H., Schroeder, F., Kier, A.B., 2002. Membrane charge and curvature determine interaction with acyl-CoA binding protein (ACBP) and fatty acyl-CoA targeting. Biochemistry 41, 10540–10553.

Chong, P.L., Capes, S., Wong, P.T.T., 1989. Effects of hydrostatic-pressure on the location of prodan in lipid bilayers—a FT-IR study. Biochemistry 28, 8358–8363.

Epand, R.F., Kraayenhof, R., Sterk, G.J., Wong Fong Sang, H.W., Epand, R.M., 1996. Fluorescent probes of membrane surface properties. Biochim. Biophys. Acta 1284, 191–195.

Fee, R.S., Maroncelli, M., 1994. Estimating the time-zero spectrum in time-resolved emission measurements of solvation dynamics. Chem. Phys. 183, 235–247.

Finer, E.G., Darke, A., 1974. Phospholipid hydration studied by deuteron magnetic resonance spectroscopy. Chem. Phys. Lipids 12, 1–16.

Heerklotz, H., Seelig, J., 2002. Application of pressure perturbation calorimetry to lipid bilayers. Biophys. J. 82, 1445–1452.

Hof, M., Hutterer, R., Perez, N., Ruf, H., Schneider, F.W., 1994. Influence of vesicle curvature on fluorescence relaxation kinetics of fluorophores. Biophys. Chem. 52, 165–172.

Hope, M.J., Bally, M.B., Mayer, L.D., Janoff, A.S., Cullis, P.R., 1986. Generation of multilamellar and unilamellar phospholipid vesicles. Chem. Phys. Lipids 40, 89–108.

Horng, M.L., Gardecki, J.A., Papazyan, A., et al., 1995. Subpicosecond measurements of polar solvation dynamics—coumarin-153 revisited. J. Phys. Chem. 99, 17311–17337.

Hutterer, R., Schneider, F.W., Sprinz, H., Hof, M., 1996. Binding and relaxation behaviour of Prodan and Patman in phospholipid vesicles: a fluorescence and ^{1}H-NMR study. Biophys. Chem. 61, 151–160.

Hutterer, R., Schneider, F.W., Hof, M., 1997a. Anisotropy and lifetime profiles for *n*-anthroyloxy fatty acids: a fluorescence method for the detection of bilayer interdigitation. Chem. Phys. Lipids 86, 51–64.

Hutterer, R., Schneider, F.W., Lanig, H., Hof, M., 1997b. Solvent relaxation behaviour of *n*-anthroyloxy fatty acids in PC-vesicles and paraffin oil: a time-resolved emission spectra study. Biochim. Biophys. Acta 1323, 195–207.

Hutterer, R., Hof, M., 2002. Probing ethanol-induced phospholipid phase transitions by the polarity sensitive fluorescence probes Prodan and Patman. Z. Phys. Chem. 216, 333–346.

Hutterer, R., Schneider, F.W., Fidler, V., Grell, E., Hof, M., 1997c. Time evolved emission spectra of Prodan and Patman in large unilamellar vesicles: a comparison between ether- and acyllipids. J. Fluor. 7, 27–33.

Huttner, W.B., Zimmerberg, J., 2001. Implications of lipid microdomains for membrane curvature, budding and fission—commentary. Curr. Opin. Cell Biol. 13, 478–484.

Klymchenko, A.S., Duportail, G., Demchenko, A.P., Mely, Y., 2004. Bimodal distribution and fluorescence response of environment-sensitive probes in lipid bilayers. Biophys. J. 86, 2929–2941.

Koynova, R., Caffrey, M., 1998. Phases and phase transitions of the phosphatidylcholines. Biochim. Biophys. Acta 1376, 91–145.

Lindblom, G., Persson, N.O., Arvidson, G., 1976. Ion binding and water orientation in lipid model membrane systems studied by NMR. In: Friberg, S., Gould, R.F. (Eds.), Lyotropic Liquid Crystals and the Structure of Biomembranes. ACS, Washington, pp. 121–141.

Sheynis, T., Sýkora, J., Benda, A., Kolusheva, S., Hof, M., Jelinek, R., 2003. Bilayer localization of membrane-active peptides studied in biomimetic vesicles by visible and fluorescence spectroscopies. Eur. J. Biochem. 270, 4478–4487.

Sterk, G.J., Thijsse, P.A., Epand, R.F., Wong Fong Sang, H.W., Kraayenhof, R., Epand, R.M., 1997. New fluorescent probes for polarity estimations at different distances from the membrane interface. J. Fluoresc. 7, 115S–118S.

Sýkora, J., Kapusta, P., Fidler, V., Hof, M., 2002a. On what time scale does solvent relaxation in phospholipid bilayers happen? Langmuir 18, 571–574.

Sýkora, J., Mudogo, V., Hutterer, R., Nepraš, M., Vaněrka, J., Kapusta, P., Fidler, V., Hof, M., 2002b. ABA-C_{15}: a new dye for probing solvent relaxation in phospholipid bilayers. Langmuir 18, 9276–9282.

Tamm, L.K., Crane, J., Kiessling, V., 2003. Membrane fusion: a structural perspective on the interplay of lipids and proteins. Curr. Opin. Cell Biol. 13, 453–466.

Westlund, P.O., 2000. Line shape analysis of NMR powder spectra of $^{2}H_2O$ in Lipid Bilayer Systems. J. Phys. Chem. B 104, 6059–6064.

Zimmerberg, J., McLaughlin, S., 2004. Membrane curvature: how BAR domains bend bilayers. Curr. Biol. 14, R250–R252.